J. Non-Newtonian Fluid Mech. 165 (2010) 340–349

Contents lists available at ScienceDirect

Journal of Non-Newtonian Fluid Mechanics

journal homepage: www.elsevier.com/locate/jnnfm

Effects of viscoelasticity on the retraction of a sheared drop

Swarnajay Mukherjee, Kausik Sarkar*

Department of Mechanical Engineering, University of Delaware, 130 Academy Street, 126 Spencer Lab, Newark, DE, United States

ARTICLE INFO

Article history:
Received 27 July 2009
Received in revised form
15 December 2009
Accepted 7 January 2010

Keywords:
Oldroyd B
Viscoelasticity
Emulsion
Relaxation
Drop
Non-Newtonian
Retraction

ABSTRACT

Effects of drop and matrix viscoelasticity on the retraction of a sheared drop are numerically investigated. Retraction of an Oldroyd-B drop in a Newtonian matrix is initially faster and later slower with increasing drop Deborah number. The observed behavior is explained using an ordinary differential equation model representing the dominant balance between various forces during retraction. The initial faster relaxation of viscoelastic drops is due to viscoelastic stresses pulling the drop interface at the tips inward. The later slower retraction is due to the slowly-relaxing viscoelastic forces at the equator, where they act against the capillary force. The drop inclination decreases substantially during retraction unlike in a Newtonian case. Matrix viscoelasticity slows the relaxation of a Newtonian drop because of the increasingly slow relaxation of highly stretched polymers near the drop tip with increasing Deborah number. Increasing the ratio of polymeric to total viscosity further accentuates the viscoelastic effects in both cases. For an Oldroyd-B drop in an Oldroyd-B matrix, a competition between the dispersed and the continuous phase elasticities, represented by their ratio, determines the dynamics; larger values of the ratio leads again to initial faster and later slower retraction.

1. Introduction

Drop deformation and its subsequent interfacial tension driven retraction after flow cessation are fundamental to the understanding of the rheological behavior of emulsions. The retraction process can also be used to measure the interfacial tension between the drop and the matrix phase, once the dynamics is mathematically related to the interfacial tension [1–4]. One would expect the material response of the drop and the matrix phases to critically affect the retraction dynamics, and therefore the measurement process. In this paper we investigate the retraction of a sheared drop when the drop and/or the matrix phases are viscoelastic.

The drop dynamics in a zero-inertia Newtonian system has been extensively studied [5–13]. In recent years two departures from this system—finite inertia [14–22] and viscoelastic constitutive equations [23–33]—have received increased attention. Unlike the Newtonian case, viscoelastic systems are poorly understood, and there are widespread controversies [29,30,34–39] (see [40] for a review). The problem lies in the subtle competition between the developing viscous and viscoelastic stresses. Therefore there is a critical need to carefully simulate such flows and develop an intuition for them comparable to the Newtonian system. We have recently developed a robust algorithm for viscoelastic system [24], and simulated drop deformation and breakup in shear when the drop or/and the matrix phases satisfy Oldroyd-B model (O/N, N/O, O/O) [40–43]. Simulation provides detailed information about the stresses, that proved critical for explaining the simulated non-monotonic response of drops to shear as well as results from earlier viscoelastic experiments [35,37].

Drop retraction method for estimating surface tension has mostly been used for polymeric liquids with substantial elasticity. Yet the analysis were based on either small deformation theory [1,3] or the Maffetone–Minale ellipsoidal drop model [2]; both theories assume a Newtonian constitutive behavior. As to drop relaxation in a viscoelastic system, Tretheway and Leal [25] performed a detailed experimental study of a Newtonian drop relaxing in a non-Newtonian fluid after a planar extensional flow was stopped. They concluded that the elastic stress developed at the boundary fundamentally changes the large deformation dynamics and retards the relaxation process. Similar retarding influence of matrix viscoelasticity is also seen in shear [44], where the authors compared experimentally observed dynamics against models proposed by Maffettone and Greco [39] and Yu et al. [32]. Numerically, Yue et al. [45] performed a two-dimensional simulation of the retraction process, and found that for an initially ellipsoidal drop shape with zero velocity and zero stress, viscoelasticity in the drop or in the matrix affects the retraction process in the same way. The drop retraction initially is faster because, as the authors suggested, the retarding viscoelastic stress is yet to develop, and after it develops it slows the retraction. However, even for the more realistic case of a sheared drop with a nonzero initial stress, they found similar visoelastic effects on the retraction dynamics for the O/N

* Corresponding author. Tel.: +1 302 831 0149.
E-mail address: sarkar@udel.edu (K. Sarkar).

0377-0257/$ – see front matter © 2010 Elsevier B.V. All rights reserved.
doi:10.1016/j.jnnfm.2010.01.008

system as that of the initially unstressed drop. The initial acceleration and eventual retardation of the retraction for a sheared drop with fully developed viscoelastic stresses therefore remains puzzling and justifies further investigation in a three dimensional setting. The matrix viscoelasticity (N/O) for an initially stressed drop affects the retraction in a much more pronounced way, and the retraction is always slower with increasing viscoelasticity. Experiments and simulation using an Oldroyd-B model performed by Verhulst et al. [46] showed that the behavior of a viscoelastic drop (O/N) does not differ much from that of a Newtonian one (N/N), whereas viscoelastic matrix (N/O) slows down the process considerably.

The drop dynamics in a viscoelastic system is a result of subtle interplay between different forces. Careful experiments and simulation of model systems are critical for understanding it. To this end, Boger fluids with controlled rheological properties have become the experimental system of choice. However, unlike simulation, experiments cannot describe the details of how the viscous and viscoelastic stresses develop in a transient flow. Transient flow has been shown to drastically alter the drop break up in a Newtonian system [47]. Drop retraction offers a simple enough transient flow which can be used to understand stress development and its effects on the flow, as we will see in this paper, which justifies the detailed three dimensional simulation of the process.

In this paper, we numerically simulate the relaxation of a sheared drop when either or both of the drop and matrix phases are Oldroyd-B. We use a 3D front tracking finite difference method similar to our previous studies. Section 2 briefly describes the method and the problem set-up. Section 3 proves convergence and compares with previous experiments. Section 4 describes the results for an Oldroyd-B drop in a Newtonian matrix (O/N), a Newtonian drop in an Oldroyd-B matrix (N/O), and an Oldroyd-B drop in an Oldroyd-B matrix (O/O). We carefully analyze the viscoelastic forces around the drop interface to explain the simulated observations. We also develop a simple ordinary differential equation (ODE) model in the Appendix A, that we believe, captures the essential dynamics of the viscoelastic stresses in the O/N retraction. Section 5 summarizes our findings.

2. Mathematical formulation and numerical implementation

The formulation and the numerical implementation based on front tracking method are sketched briefly here as they are discussed in detail before [24,41]. The system is governed by the mass and the momentum equations:

$$\nabla \cdot \boldsymbol{u} = 0, \qquad \frac{\partial(\rho \boldsymbol{u})}{\partial t} + \nabla \cdot (\rho \boldsymbol{u}\boldsymbol{u}) = \nabla \cdot \boldsymbol{\tau} - \int_{\partial B} dx_B \kappa \boldsymbol{n} \Gamma \delta(x - x_B), \tag{1}$$

in the entire computational domain. ρ is the density, p is the pressure, Γ is the interfacial tension between the drop and the matrix phase, ∂B is the drop surface consisting of the points x_B, and κ, the local curvature. $\mathbf{n}$ represents the outward normal on the drop surface, and $\delta(x - x_B)$ is the three dimensional Dirac delta function. The total stress tensor τ is given by:

$$\begin{aligned} &\tau = -p\boldsymbol{I} + \boldsymbol{T}^p + \boldsymbol{T}^v, \quad \boldsymbol{T}^v = \mu_s \boldsymbol{D}, \\ &\lambda \left\{ \frac{\partial \boldsymbol{T}^p}{\partial t} + \boldsymbol{u} \cdot \nabla \boldsymbol{T}^p - (\nabla \boldsymbol{u})\boldsymbol{T}^p - \boldsymbol{T}^p (\nabla \boldsymbol{u})^T \right\} + \boldsymbol{T}^p = \mu_p \boldsymbol{D}, \end{aligned} \tag{2}$$

where μ_s is the solvent viscosity and $\mathbf{D} = (\nabla \mathbf{u}) + (\nabla \mathbf{u})^T$ is the strain rate tensor. $\mathbf{T}^p$ is the viscoelastic stress due to the presence of polymer and, as shown, satisfies Oldroyd-B equation. μ_p is the polymeric viscosity, and λ is the relaxation time. The superscript T represents the transpose. Note that our choice of constitutive equation despite its problem in extensional flows is based on its simplicity. For the Deborah numbers considered here, we did not see any change in basic behavior with introduction of a finite limit on the polymer extension.

The moving drop interface or the front is discretized by triangular elements. The material properties, such as ρ, μ and λ that might be different in the matrix and the drop phase (in this paper, density and viscosity are the same in both phases), are represented as smoothly varying over a few grid spacings across the interface. The interfacial tension force shown as a singular volume force in Eq. (1) is also similarly distributed over a finite thickness around the interface. Once such a smoothed version of the system is obtained, it is solved using an explicit operator splitting/projection-based finite difference method on a regular staggered Cartesian grid. The front is updated using an interpolated velocity on the front grid. Adaptive regridding is used to avoid excessive distortion of the front elements. An elastic/viscous stress splitting scheme is used for the upper convected derivative [24,41]. The pressure Poisson equation is solved using a multigrid method. An ADI method is used to avail a larger time step.

A spherical drop of radius a is placed in a computational domain of size $L_x = 10a$, $L_y = 10a$ and $L_z = 5a$, with a grid resolution of $98 \times 98 \times 49$ (grid convergence is discussed below). Velocities U and $-U$ are imposed on the upper and the lower y-boundaries respectively to create a free shear $\dot{\gamma} = 2U/L_y$. The flow is stopped after the drop has reached a steady shape, and then the drop is allowed to relax. We use a and $\tau_{ca} = \mu_m/(\Gamma/a)$ to non-dimensionalize length and time. The relevant non-dimensional parameters are Reynolds number $Re = \rho_m a^2 \dot{\gamma}/\mu_m$, capillary number $Ca = \tau_{ca}\dot{\gamma}$, Deborah number $De = \lambda\dot{\gamma}$, viscosity ratio $\lambda_\mu = \mu_d/\mu_m$, density ratio $\lambda_\rho = \rho_d/\rho_m$ and $\beta = \mu_{pd}/\mu_d$ or $\beta = \mu_{pm}/\mu_m$—the ratio of the polymeric viscosity to the total viscosity. Subscripts m and d correspond to the matrix and the dispersed phase respectively. Because the code is explicit, the code cannot simulate Stokes flows; simulations are performed at $Re = 0.1$ representative of a small Reynolds number case (see Section 3). The total viscosity is $\mu_d = \mu_{sd} + \mu_{pd}$ or $\mu_m = \mu_{sm} + \mu_{pm}$, sum of the solvent and polymeric viscosities. In the interest of brevity, we restrict the computation to $\lambda_\rho = \lambda_\mu = 1$ and $Ca = 0.3$ (drops do not break up but attain a moderate deformation at this capillary number). Note that viscosity ratio does affect significantly drop deformation in a viscoelastic system [43]. The value of β is 0.5 for all the computations, except where we study the effect of β variation. We use the Taylor criterion $D = (L - B)/(L + B)$ as a measure for drop deformation, with L and B being the semi-major and semi-minor axes of the drop. In our simulation $t' = t/\tau_{ca} = 0$ coincides with the time when the shear has been switched off.

3. Convergence study and comparison with previous work

As mentioned above, the drop is first deformed by a constant shear, and after it reaches a steady shape, the shear is stopped. As our simulations are at $Re = 0.1$, inertia introduces a finite relaxation time for the velocity profile, i.e. after the velocity boundary conditions at the upper and the lower boundaries are changed, unlike in Stokes flow, it takes a finite time to affect the overall flow field. Therefore, along with the change in velocity boundary conditions, we also subtract the shear velocity $\dot{\gamma}y$ in the entire flow field at $t' = 0$ (a simple shear (without any drop) would instantaneously relax in a Stokes flow when the bounding plates are stopped). In Fig. 1(a) we plot D vs. t' for $Ca = 0.14$ and $p = 0.5$, where $p = De/Ca$ (for validation, we use p to characterize as in ref [44]) with and without this subtraction. The simulation without subtraction shows a finite lag but otherwise they are similar. Inclination angle evolution in the inset of Fig. 1(a) shows a similar lag for the unmodified simulation. Subtracting $\dot{\gamma}y$ from the velocity profile changes $\nabla \mathbf{u}$ (particularly

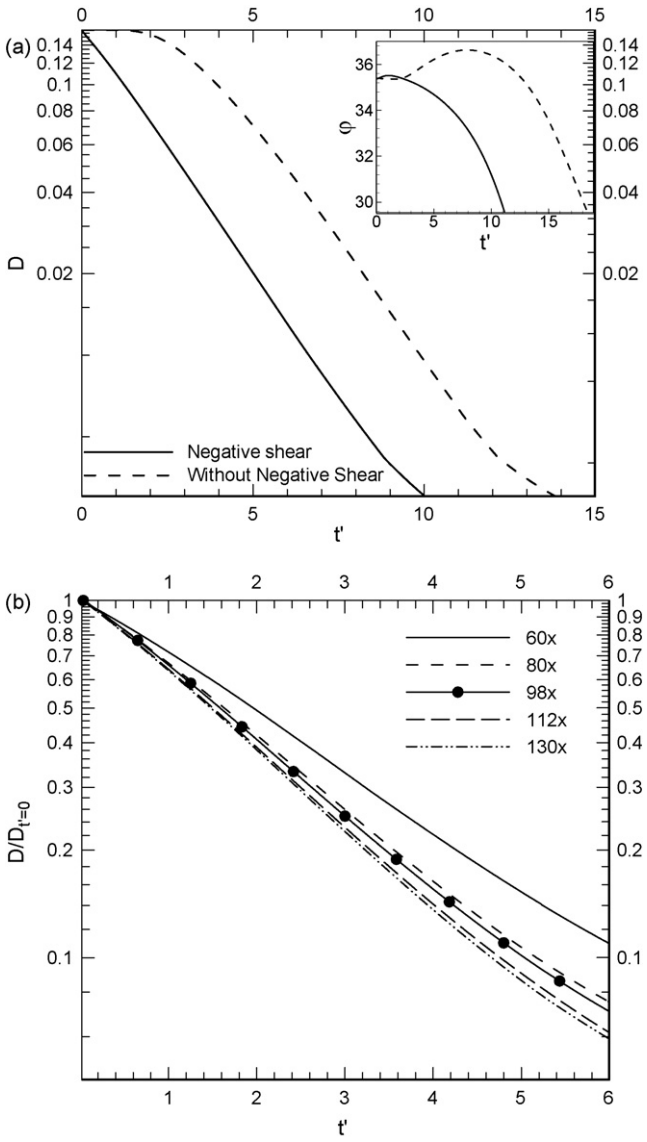

Fig. 1. (a) Comparison of transient deformation of a viscoelastic drop in a Newtonian matrix for $Ca = 0.14$, $p = 0.5$, $\lambda_\mu = 1$ with and without subtracting $\dot{\gamma}y$ from the flow when the flow is stopped. Inset shows the variation of inclination angle with time for the same data. (b) Deformation D normalized by the steady state value (at $t' = 0$) with varying discretization level from $80 \times 80 \times 40$ (80×) to $130 \times 130 \times 80$ (130×) for $Ca = 0.3$, $De_d = 2$ and $\lambda_\mu = 1$.

the $\partial u/\partial y$ term) abruptly. To ensure that the simulation results are correct, deformation, inclination and force plots (based on which we explain our results) are computed with and without subtracting $\dot{\gamma}y$ and found to be similar except for the finite time lag. Furthermore, as discussed below, the procedure is able to match with an analytical solution for the Newtonian system (see Fig. 2) making us confident about the code.

We have established computational convergence for Oldroyd-B algorithm in the previous studies both for viscosity matched [40,41] and unmatched [43] systems. In Fig. 1(b) we plot the transient evolution of deformation parameter of an Oldroyd-B drop relaxing in a Newtonian matrix by varying the discretization level from $60 \times 60 \times 30$ to $130 \times 130 \times 65$ showing very little variation beyond $80 \times 80 \times 40$. In the interest of achieving a reasonable computational time, the $98 \times 98 \times 49$ resolution is chosen for our study.

To estimate the interfacial tension using the time-dependent relaxation of drops, Luciani et al. [1] used an equation due to Rallison [7]

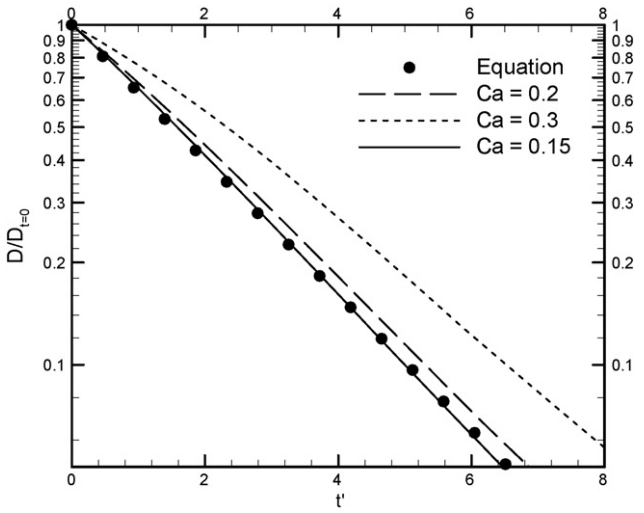

Fig. 2. Deformation of a retracting Newtonian drop in a Newtonian matrix at varying capillary numbers: comparison of simulation and small deformation analytical model (Eq. (3)).

$$D = D_o \exp\left[-\frac{40(\lambda_\mu + 1)}{(2\lambda_\mu + 3)(19\lambda_\mu + 16)}\left(\frac{\Gamma}{\mu_m a}\right)t\right], \tag{3}$$

where D_o is the initial deformation (when the shear was stopped). Our simulation at $Ca = 0.15$ matches extremely well with Eq. (3) which is valid for small deformation (Fig. 2). For higher capillary numbers, deformation is large and the simulation deviates from the analytical relation.

Data for drop retraction for viscoelastic cases are limited in the literature. In Fig. 3 we compare our simulation with experimental [44] and analytical [39] results for a Newtonian drop retracting in a viscoelastic matrix. Our simulation matches very well with the experimental results till $t' \approx 2$ for $Ca = 0.14$, $p = 0.5$ where $p = De/Ca$, and beyond that time the experimental result relaxes more slowly; this may be due to the inability of the models (Oldroyd-B equation or second-order fluid for the Maffetone and Greco model) to accurately describe the matrix liquid. The analytical curve is

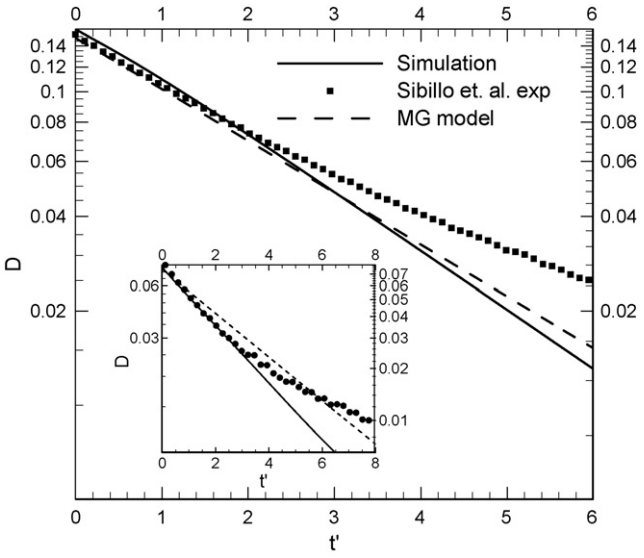

Fig. 3. Comparison of simulation with experiments by Sibillo et al. [28] and Maffettone–Greco (MG) model for a Newtonian drop retracting in a viscoelastic matrix at $Ca = 0.14$, $p = 0.5$, $\lambda_\mu = 1$, and (in the inset) $Ca = 0.07$, $p = 1.4$, $\lambda_\mu = 1$.

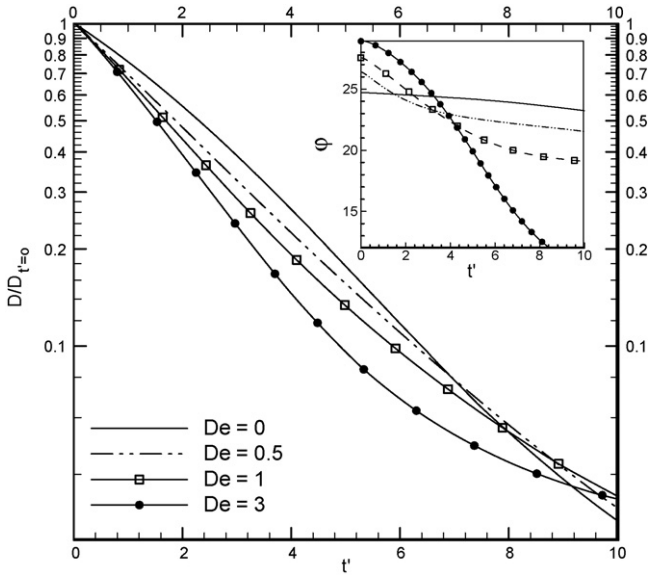

Fig. 4. Deformation of a viscoelastic drop in a Newtonian matrix normalized by its initial value at $Ca = 0.3$ for different De_d. Inset shows inclination angle of the drop for the same cases.

very close to our simulation. For $Ca = 0.07$, $p = 1.5$ (Fig. 3 inset), our simulation again corresponds well to the initial trend of the experimental results (till $t' \approx 3$), and then deviates a little. The analytical result is slower than the simulation and the experiment, latter two matching in the initial part of the evolution. Later the experimental observation seems to suggest a slowing down of the drop retraction. Note that the analytical model due to Maffettone–Greco (MG) [39] is based on a second-order fluid model different from Oldroyd-B. Based on these tests, we are reasonably certain about the accuracy of our numerical method for simulating drop retraction.

4. Results and discussion

4.1. Oldroyd-B drop in a Newtonian matrix (O/N)

In this section we investigate the transient deformation of an Oldroyd-B drop relaxing in a Newtonian matrix. As mentioned before, the study in this paper is restricted to the case of $Ca = 0.3$, which leads to moderate deformation and yet the drop remains bounded. Fig. 4 plots the transient deformation normalized by its initial value (when the retraction starts) for various Deborah numbers. We see that with higher De_d (higher relaxation time), drops initially retract quickly as compared to drops with lower De_d values. However after a certain period of time, we notice a trend reversal—slowing down of the relaxation process, the effect increasing with increasing De_d. Such a trend reversal was also noted in recent two-dimensional simulation [45], both for initially stress-free ellipsoidal drops and for sheared drops with viscoelastic stresses at $t' = 0$, developed during shearing. For the initially unstressed drops, the authors ascribed the phenomenon to the finite time needed for development of the viscoelastic stresses that impede deformation. However, the persistence of the phenomenon in the case of drops with initial viscoelastic stresses presents a puzzle, and needs careful scrutiny of the evolution of stresses.

Plot of the inclination angle in the inset of Fig. 4 for the same cases shows an interesting feature in that, while a Newtonian drop relaxes to its spherical shape without any change in its inclination, a viscoelastic drop changes its inclination during retraction. A viscoelastic drop achieves a higher inclination angle than its Newtonian counterpart during shear, but during retraction, the angle decreases and the rate of decrease is higher for higher De_d reaching finally lower than the N/N inclination. One should however be careful that at the later stage of the process, the angle is hard to determine for a nearly spherical drop. Note that the angle change is clearly due to the persistence of the memory of the original shear through the viscoelastic stresses. For an ellipsoidal drop with zero initial stress and velocity, the drop axis does not change its inclination (not shown here).

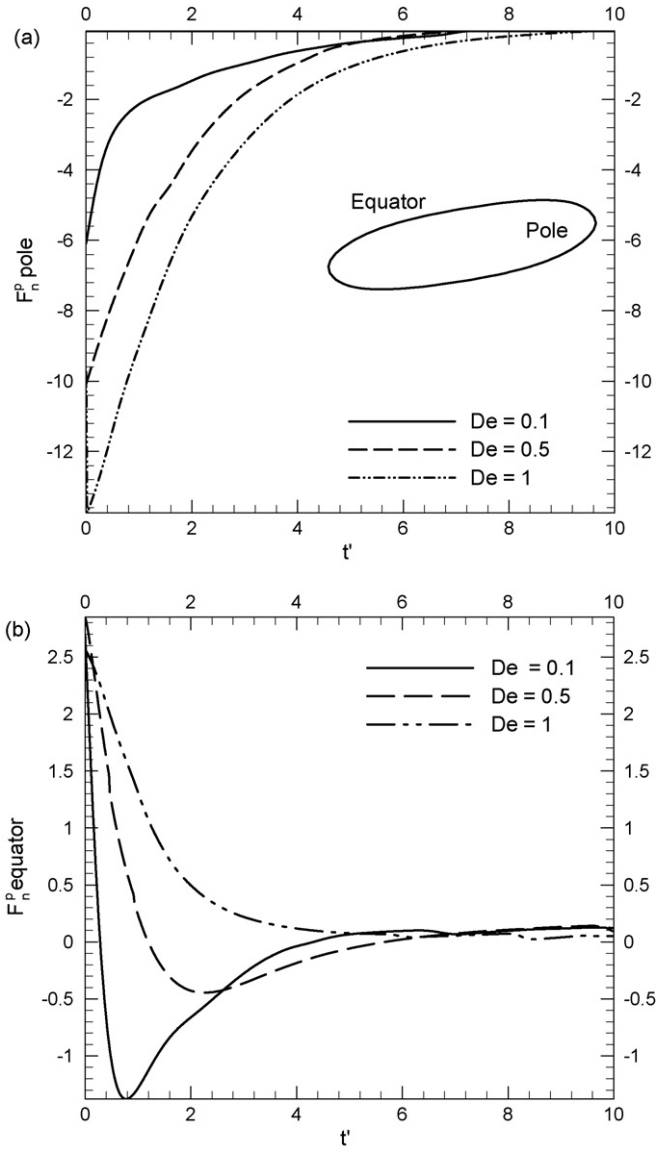

Fig. 5. Viscoelastic normal force ($F_n^p = \boldsymbol{n} \cdot (\nabla \cdot \boldsymbol{T}^p)$) at the (a) pole and the (b) equator for a viscoelastic drop in a Newtonian matrix at $Ca = 0.3$ with varying De_d.

In Fig. 5(a) and (b), we plot the force $F_n^p = \boldsymbol{n} \cdot (\nabla \cdot \boldsymbol{T}^p)$ due to elastic stress at the pole (drop tip) and the equator respectively. ($\nabla \cdot \mathbf{T}^p$ is the force that a fluid element feels per unit volume due to elastic stress, and appears in the momentum Eq. (1). In the Newtonian limit ($De_d \to 0$), the extra stress $\mathbf{T}^p$ becomes $\mu_p D$. From Fig. 5(a) we see that the elastic normal force at the pole is compressive, i.e. trying to reduce L, which results in a lower deformation for the viscoelastic drop with increasing De_d. It results in quicker initial relaxation with increasing Deborah number (Fig. 4). On the other hand, elastic force at the equator shows a non-monotonic behavior in Fig. 5(b). For low Deborah numbers—as soon as the shear stops, it falls sharply from its original positive (tensional) value and for lower De_d to a negative minimum and then grows to eventually reach zero. The minimum becomes more negative as De_d is

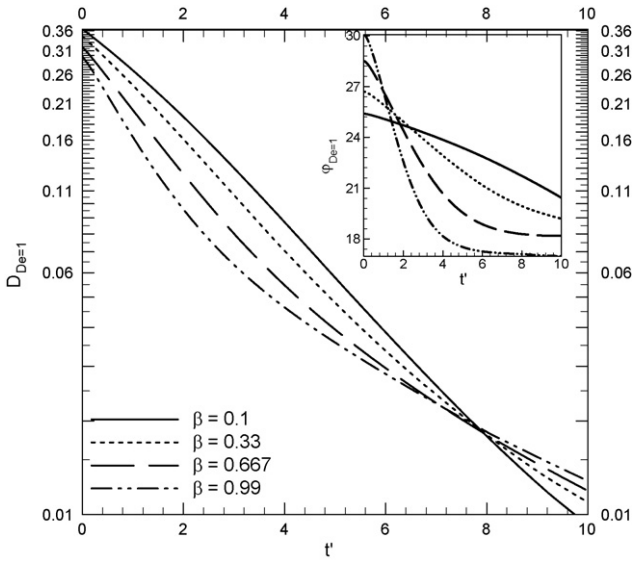

Fig. 6. Viscoelastic drop retracting in a Newtonian matrix for varying $\beta(=\mu_{pd}/\mu_d)$ at $Ca = 0.3$ and $De_d = 1.0$. Inset shows the inclination angle of the drop with the flow-axis for the same cases.

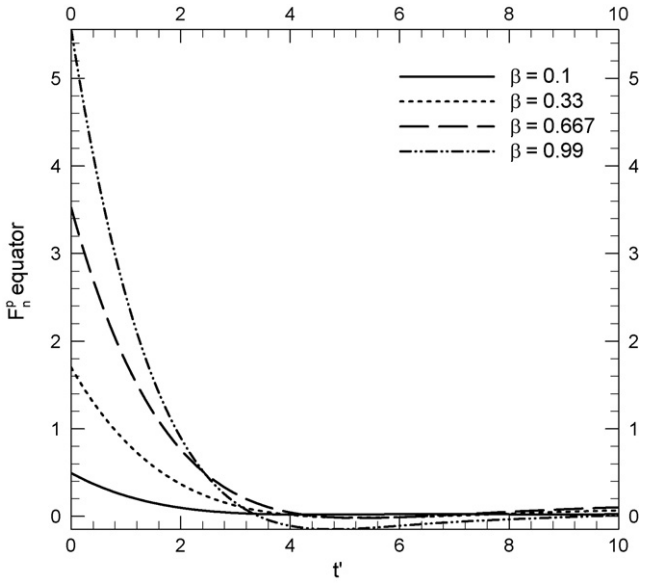

Fig. 7. Viscoelastic normal force ($F_n^p = \boldsymbol{n} \cdot (\nabla \cdot \boldsymbol{T}^p)$) at the equator of a viscoelastic drop retracting in a Newtonian matrix at $Ca = 0.3$ and $De_d = 1$ with varying β.

decreased. A negative, i.e. compressive force at the equator hinders retraction. At the start of relaxation, with increasing De_d, decreasing compressive force quickens retraction. However, at later time, one sees lower compressive force for higher De_d, e.g. force is smaller for $De_d = 0.5$ than for $De_d = 0.1$. This force at the equator explains the later slower retraction at higher De_d. Below we will provide a simple model for the phenomenon.

Next we investigate the effect of relative amount of drop viscoelasticity by varying β keeping total viscosity as well as other parameters constant. In Fig. 6 we plot deformation parameter vs. time for $Ca = 0.3$ and $De_d = 1$ for various β. For a very low value $\beta = 0.1$, the retraction is almost linear (on a semi-log plot) similar to a Newtonian drop. Increasing β makes the process non-linear. Drops with higher β initially retract quickly, but at later time, become progressively slower with lower β cases relaxing in less time. Fig. 6 inset shows faster relaxation of inclination angle with time, as the drop viscoelasticity increases. Note that even though the behavior with β variation is similar to that with Deborah variation, the detail is different. For different β, the crossover between different curves takes place around the same time because the same De_d value leads to the same time scale for these cases. Because we noted that eventual retardation of the retraction is dominated by the force at the equator, in Fig. 7, we plot time evolution of F_n^P at the equator for the same data of Fig. 6. For higher β, polymeric forces are higher (compressive at the pole and tensional at the equator); initially they result in increased rate of retraction for increased β, and later, force curves for different β cross over to indicate that the forces for lower β cases become more effective making them relax in less time.

In an attempt to understand how the viscoelastic stresses affect the retraction process, specifically what causes the faster initial retraction and latter slowing down of viscoelastic drops, we create a toy model (detailed in the Appendix A) that embodies the dominant force balance. The model is based on the fact that the flow during the retraction is roughly extensional with compression along the pole (x' axis) and extension along the equator (y' axis) (see Fig. 8). Therefore the dominant viscoelastic stresses are $\hat{T}^P_{x'x'}$ and $\hat{T}^P_{y'y'}$ which would concurrently relax along with the drop. This is modeled by Eqs. (A.5)–(A.7) presented in the Appendix A. For the initial condition on stresses in the model, we use volume averages from the simulation. We show the evolution of stresses as well as the normalized deformation in Figs. 9 and 10. Because the toy model just has representative terms for different forces, only a qualitative comparison between the model and simulation is possible. We see that the model predicts the initial faster relaxation followed by slower one for higher De_d (Fig. 9a). Furthermore, the evolution of stresses (Fig. 9b and c) from the toy model is seen to show behavior similar to those from the simulation, giving further credence to the model. Initially positive $\hat{T}^P_{x'x'}$ first reduces to a negative value and then rises to become zero. $\hat{T}^P_{y'y'}$ behaves in an exact opposite way: it has a small negative value at the start of retraction, it increases to become positive, and then decreases to zero. Eqs. (A.6) and (A.7) explain this behavior—the $2\hat{\beta}X$ term (representative of $\mu_p \mathbf{D}$ in Eq. (2)) initially dominates to reduce $\hat{T}^P_{x'x'}$ and increase $\hat{T}^P_{y'y'}$. The strain rate is proportional to the deformation and reduces with it, and in later times, stresses exponentially reduce to zero governed by Eqs. (A.6) and (A.7) with zero right-hand sides. Note also that for even-

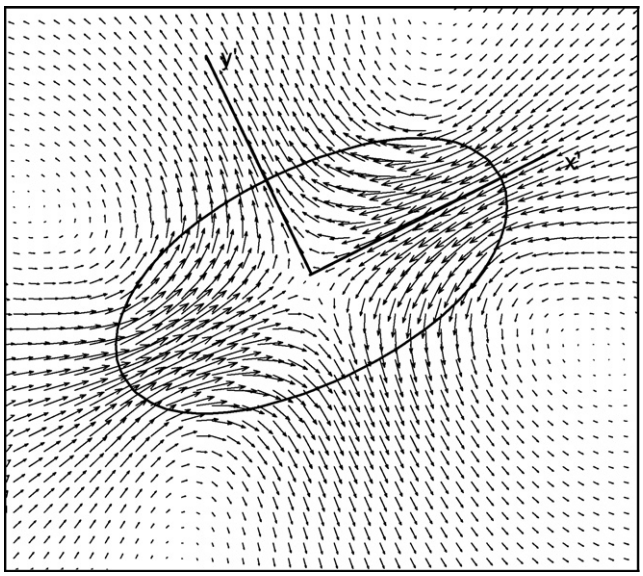

Fig. 8. Velocity field around a retracting viscoelastic drop shows an extensional flow.

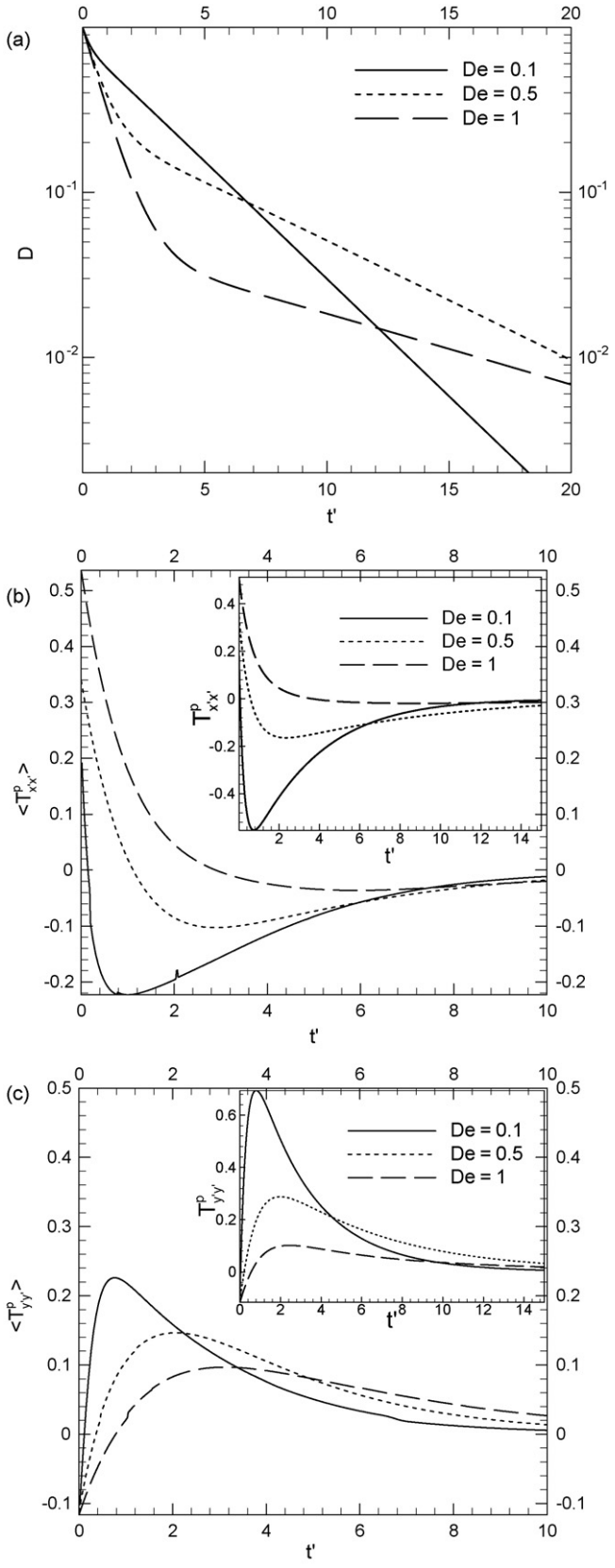

Fig. 9. (a) Deformation of a viscoelastic drop retracting in a viscoelastic matrix predicted by an ODE model for different De_d. (b) Evolution of $T^p_{x'x'}$ from the simulation and the model (inset) for the same cases. (c) Evolution of $T^p_{y'y'}$ from the simulation and the model (inset) for the same cases. The simulations are at $Ca = 0.3$.

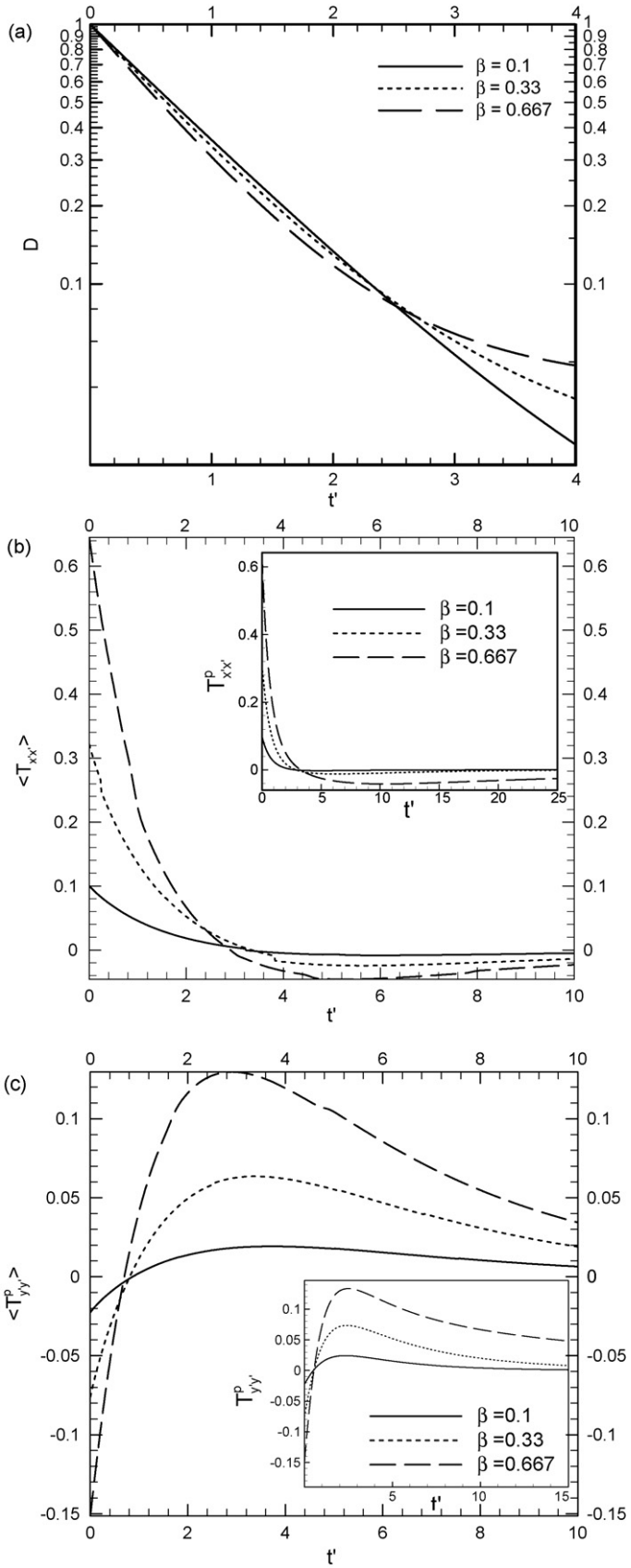

Fig. 10. (a) Deformation of a viscoelastic drop retracting in a viscoelastic matrix predicted by an ODE model for different β. (b) Evolution of $T^p_{x'x'}$ from the simulation and the model (inset) for the same cases. (c) Evolution of $T^p_{y'y'}$ from the simulation and the model (inset) for the same cases. The simulations are at $Ca = 0.3$.

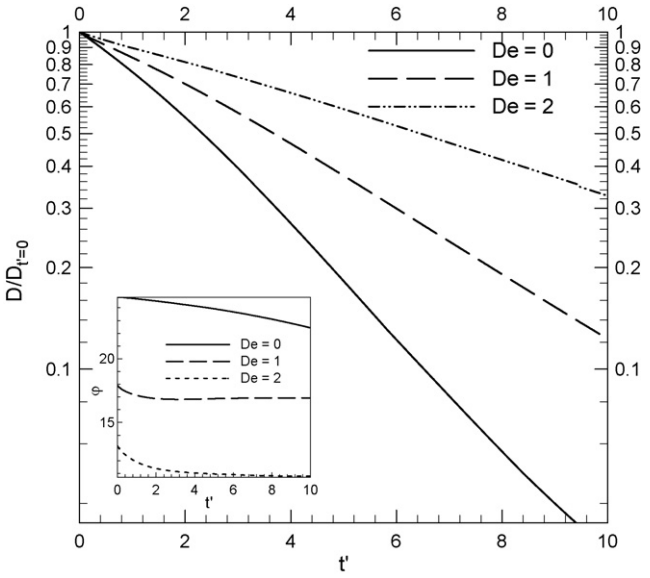

Fig. 11. Deformation and inclination angle (inset) of a retracting Newtonian drop in a viscoelastic drop for varying De_m at $Ca = 0.3$.

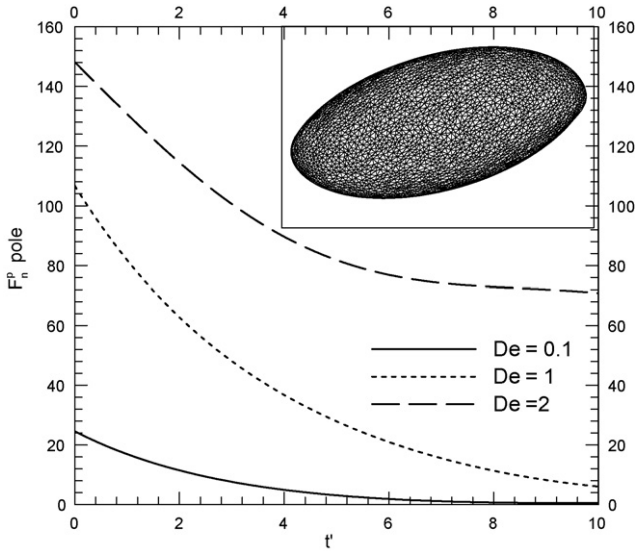

Fig. 12. Viscoelastic normal force ($F_n^p = \boldsymbol{n} \cdot (\nabla \cdot \boldsymbol{T}^p)$) at the pole for a Newtonian drop retracting in a viscoelastic matrix at $Ca = 0.3$ with varying β. Inset shows a sheared Newtonian drop in an Oldroyd-B matrix for $Ca = 0.3$, $De = 2.5$ and $\beta = 0.75$.

tually a positive $\hat{T}^P_{y'y'}$, both terms in the right-hand side in (A.7) retard its decay. However in (A.6) the second term in right-hand side is aiding the decay of $\hat{T}^P_{x'x'}$, while the response of the other term depends on the sign of $\hat{T}^P_{x'x'}$. We also note that both stresses reach extremum (minimum for $\hat{T}^P_{x'x'}$ and maximum for $\hat{T}^P_{y'y'}$) at $(\hat{T}^P_{x'x'})^{\min} = -2\beta X/(1+2DeX)$ and $(\hat{T}^P_{y'y'})^{\max} = 2\beta X/(1-2DeX)$. We note that $|(\hat{T}^P_{y'y'})^{\max}| > |(\hat{T}^P_{x'x'})^{\min}|$. These observations explain that in later time while decaying to zero, $\hat{T}^P_{y'y'}$ is larger in magnitude than $\hat{T}^P_{x'x'}$, and therefore, primarily responsible for the eventual slowing down of the retraction process. The model Eq. (A.5) predicts that the retraction in the N/N case is exponential with a capillary time scale. For viscoelastic drops, initially the high positive $\hat{T}^P_{x'x'}$ (as well as the small negative $\hat{T}^P_{y'y'}$) results in the faster decay in the deformation with increasing Deborah number. However at later times, the higher $\hat{T}^P_{y'y'}$ slows down the retraction for higher Deborah number cases, according to (A.5). In Fig. 10, we show the same cases at $De_d = 1$, but with varying β. Once again, we see similar evolution of stresses both from the model and the simulation. At higher β, $\hat{T}^P_{x'x'}$ is higher and leads to quicker relaxation initially. However, for the reason given above, $\hat{T}^P_{x'x'}$ relaxes quickly (Fig. 10b), and eventually $\hat{T}^P_{y'y'}$ dominates (Fig. 10c). Higher $\hat{T}^P_{y'y'}$ for higher β retards the relaxation process more effectively at later times, which leads to a crossing of the model deformation curves for different β (Fig. 10a) similar to the simulation (Fig. 6). For an initially ellipsoidal viscoelastic drop with zero initial stresses, simulation leads to similar behavior—initially faster and later slower retraction—as was also seen in 2D simulation before [45]. We do not show it in the interest of brevity. The ODE model was also able to predict it. We note that the results showing change in trend and other subtle variations are because of the complex evolution and the interplay of different viscoelastic stresses. They are the reason for contradictory results in the literature for drop deformation in viscoelastic systems [41].

4.2. Newtonian drop in Oldroyd-B matrix (N/O)

Next we investigate the deformation of a Newtonian drop in an Oldroyd-B matrix. In Section 3, we saw that our simulation reasonably matches with the experimental results. In Fig. 11, D vs. time shows that increasing matrix viscoelasticity increasingly slows down the retraction. Sibillo et al. [44] experimentally noticed similar slowing down of drop retraction by matrix viscoelasticity. Fig. 11 inset plots the inclination angle φ for the same cases. Increasing matrix viscoelasticity leads to lower inclination angle for a sheared drop. During relaxation, it does not change much.

Polymeric force F^P_n at the pole in Fig. 12 shows that it is tensional and opposite to that in the O/N case. Force at the equator (not shown) is an order of magnitude smaller than that at the pole. Therefore, the force at the pole is primarily responsible for the process, and the retarded relaxation is far easily explained compared to the O/N case. The tensional force at the pole hinders retraction, and being higher for higher De_m, slows retraction more effectively. In fact, the effect of matrix viscoelasticity is much more pronounced compared to that of the drop. Tretheway and Leal [25] in their study of drop retraction in an extensional flow suggested that the increased tensile stress induced by the contraction of the drop poles causes the retardation of the retraction process in a viscoelastic matrix. This is in accordance with our finding of extremely high viscoelastic forces at the pole. They observed pointed drop tips for drops deforming in a viscoelastic matrix and attributed the effect to local extension of polymers because of non-linear interaction between drop shape change, flow modification and polymer configuration. We also see pointed drop tips (inset of Fig. 12).

In Fig. 13, we see that the relaxation is also retarded with increasing β at the same $De_m = 1$. However, the effect is not as pronounced as changing De_m. The inset of Fig. 13 shows that the normalized deformation parameter at non-dimensional times 2 and 4 increases linearly with β. This can be explained by noting that the retarding viscoelastic stress in the matrix is linear with β. Therefore, a decay equation for deformation such as (A.5) with only such a retarding stress at the pole would result in a deformation varying linearly with β.

4.3. Oldroyd-B drop in Oldroyd-B matrix (O/O)

We briefly investigate the effects of viscoelasticity when both the phases considered are viscoelastic. Such systems have been experimentally investigated by Mighri et al. [37] where they used Boger fluids with four different relaxation times. They concluded opposite effects of drop and matrix elasticity on deformation;

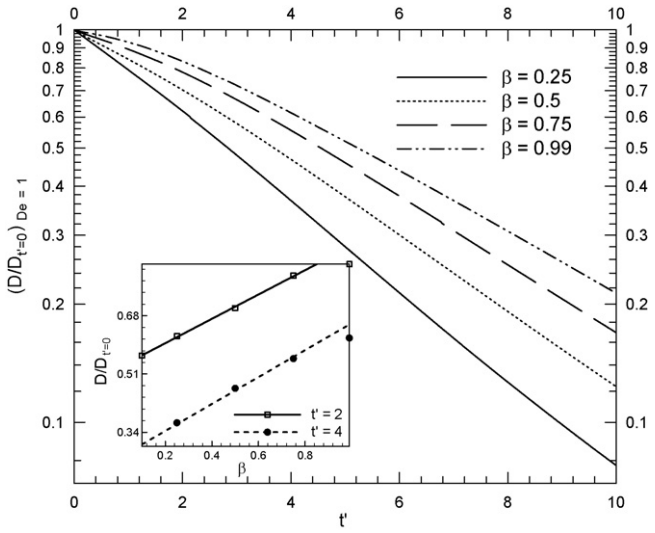

Fig. 13. Deformation normalized with the steady state value of a Newtonian drop retracting in a viscoelastic matrix for varying β at $Ca = 0.3$ and $De_m = 1.0$. Inset shows the normalized deformation with β at $t' = 2$ and $t' = 4$.

increasing the elasticity parameter $k = \lambda_d/\lambda_m = De_d/De_m$ decreases drop deformation. Aggarwal and Sarkar [40] observed a monotonic decrease in steady state value of D (D_{steady}) with k. They also observed that D_{steady} in the O/O case is lower than that of the fully Newtonian system for smaller values of De_m while for higher De_m (e.g. $De = 2.0$), D_{steady} is higher than that of the Newtonian case for small k.

In the previous two sections we observed that viscoelasticity in either phase delays drop retraction; delaying of the retraction due to matrix elasticity is very prominent right from the beginning whereas drop viscoelasticity quickens retraction initially but slows down the process eventually. So we expect that in O/O case, retraction would be slower eventually as De is increased for either phase. However, initially there is a competition between the elastic effects of two phases. Initially drop elasticity tries to retract the drop quickly while matrix elasticity tries to slow it down. In Fig. 14(a) we plot deformation parameter normalized by its initial steady value for $Ca = 0.3$ for various $k = \lambda_d/\lambda_m = De_d/De_m$ while keeping $De_m = 1.0$. As k is increased the drop viscoelastic effects increase, and we see a quicker relaxation for the initial period followed by slowing down at later time similar to the O/N case. We investigate the normal forces at the pole and the equator in Fig. 14(b) and (c). They resemble those for N/O case (see Fig. 12) indicating that the viscoelasticity of the matrix dominates that of the drop. At the pole, drops with higher k have lower positive force, i.e. more inward pull due to viscoelastic stresses inside the drop. Consequently, higher k means quicker relaxation. However at later times, the forces at the equator (Fig. 14c) become dominant as for the O/N case; for higher k, the higher compressive force at the equator delays the retraction eventually.

5. Summary

We numerically simulate the retraction of a drop when either or both of the matrix and drop phases are modeled by an Oldroyd-B equation. The simulation compares well with previous experiments and analytical models. Increasing drop phase Deborah number initially accelerates the drop retraction, but later slows it down. Increasing the matrix phase Deborah number slows down the relaxation process right from the beginning. Due to the viscoelastic stresses developed during the shearing, the drop inclination angle was seen to change during retraction. For the Oldroyd-B drop in

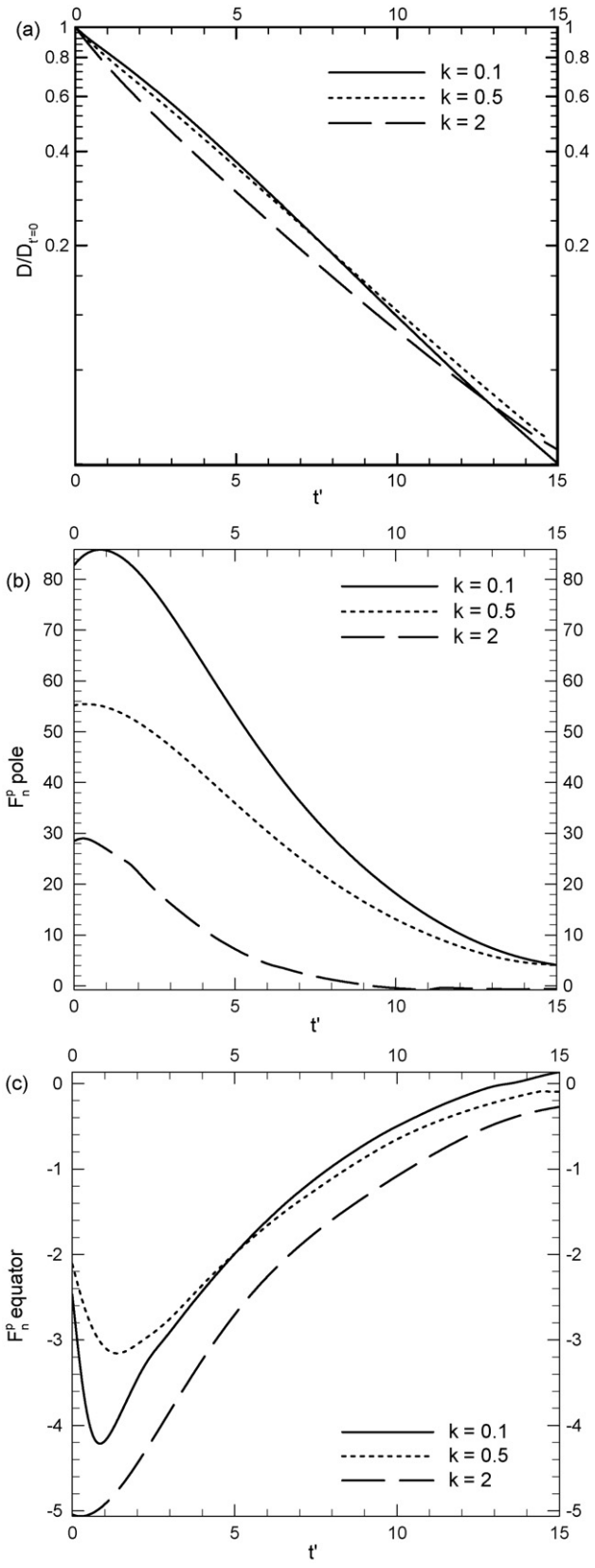

Fig. 14. Deformation (a) and normal forces at the pole (b) and equator (c) for a viscoelastic drop retracting in a viscoelastic matrix with varying k at $De_m = 1.0$ and $Ca = 0.3$.

a Newtonian matrix, the non-monotonic behavior is explained by resorting to a simple model. It assumes the flow for the retracting drop to be roughly extensional, and involves three ODEs for the two principle viscoelastic stresses and the deformation. The model predicts the qualitative behavior of the simulated stresses and the deformation. It shows that the tensional visoelastic stress primarily acting at the pole is clearly aiding the capillary stress in retracting the drop. However, the stress at the equator is opposing the retraction and leads to eventual slowing down. For a Newtonian drop in an Oldroyd-B matrix, the force at the pole due to stretched polymers inhibiting the retraction is much stronger and gives rise to the delayed response. Increasing the ratio of the polymeric viscosity to the total viscosity of the viscoelastic phase leads to deformation variation similar to that due to increasing Deborah number. Retraction of an Oldroyd-B drop in an Oldroyd-B matrix is determined initially by the competition of the quickening influence of the drop viscoelasticity and the retarding influence of the matrix viscoelasticity.

The investigation shows that viscoelasticity in a relatively simple situation such as the relaxation of a sheared drop can give rise to complex dynamics as a result of subtle interplay between developing viscoelastic stresses. Computation in conjunction with simple approximate models can be a powerful tool in explaining the underlying physics. Finally, for estimating the surface tension from drop retraction, the current analysis shows the difficulties when either phase is viscoelastic. Even the simple toy model that was employed to explain the dynamics requires three evolution equations. Relating the retraction to measurable rheological properties (e.g. shear dependent viscosity, normal stress differences) of the two phases by simple algebraic correlation (at least in certain range of parameters) will be of use and remains a challenge for future work.

Acknowledgements

Authors are grateful to Professor Stefano Guido for providing his experimental data. KS acknowledges financial support from NSF grant CBET-0625599.

Appendix A.

For the Oldroyd-B drop relaxing in a Newtonian matrix, we find that the drop viscoelasticity leads to faster drop relaxation initially and latter a slowing down. In an attempt to understand it we develop a simple model. For the drop, we use a model similar to what has been used in our previous articles [15,41]:

$$\hat{\mu}\hat{a}^2\dot{X} + \hat{\sigma}\hat{a}X + (\hat{T}^p_{xx} - \hat{T}^p_{yy})\hat{a}^2 = 0, \quad X(0) = 1. \tag{A.1}$$

Here X represents the non-dimensional drop deformation. Each term is a force acting on an area a^2. The first term is representative of the viscous 'damping'. The second term represents the interfacial contribution $\Delta\hat{p} \sim \hat{\sigma}/[\hat{a}(1+X)] \approx \hat{\sigma}(1-X)/\hat{a}$ ($\hat{\sigma}/\hat{a}$ just gives rise to an isotropic pressure). The third term is the viscoelastic stresses. Note that we assume that the flow inside the drop is roughly extensional with the x'-axis of extension towards the pole (as can be seen from simulation in Fig. 9). For the viscoelastic stresses, we use Eq. (2). In an extensional flow, all off-diagonal strain rate terms are zero. Therefore, for an Oldroyd-B fluid, the viscoelastic stresses (2) become

$$\lambda\left[\frac{\partial T^p_{x'x'}}{\partial t} - 2T^p_{x'x'}\frac{\partial u'}{\partial x'}\right] + T^p_{x'x'} = 2\mu_p\frac{\partial u'}{\partial x'}, \tag{A.2}$$

$$\lambda\left[\frac{\partial T^p_{y'y'}}{\partial t} - 2T^p_{y'y'}\frac{\partial v'}{\partial y'}\right] + T^p_{y'y'} = 2\mu_p\frac{\partial v'}{\partial y'}, \tag{A.3}$$

$$\lambda\left[\frac{\partial T^p_{z'z'}}{\partial t} - 2T^p_{z'z'}\frac{\partial w'}{\partial z'}\right] + T^p_{z'z'} = 2\mu_p\frac{\partial w'}{\partial z'}, \tag{A.4}$$

Initially the sheared drop will start its relaxation with stresses (at $t' = 0$) that it has accrued during shearing. The advection terms are not included above with an understanding that the stresses are average over the drop volume V_0. For the initial conditions on stresses for the model, we use

$$\langle \boldsymbol{T}^p \rangle = \frac{\int_{V_0} \boldsymbol{T}^p \, dV}{V_0}$$

from the simulation. We have found numerically that $T^p_{z'z'}$ remains small during the entire relaxation process. Therefore, we neglect it in the spirit of dominant balance. For the model, we use symbols with hat to distinguish them from those in the simulation. For the velocity gradients in (A.3) and (A.4), we note that the extensional flow is generated by the deforming drop. Therefore $\partial u'/\partial x' \sim -\partial v'/\partial y' \sim -X$. This can be further justified by noting that in a purely viscous system with the elastic stress terms from (A.1), $X \sim e^{-t\hat{\sigma}/\hat{\mu}\hat{a}}$, insinuating an exponentially relaxing strain rate. We non-dimensionalize (with a and $\dot{\gamma}^{-1}$) the equations to obtain

$$\frac{dX}{dt} + \frac{1}{\hat{C}a}X + (\hat{T}^p_{x'x'} - \hat{T}^p_{y'y'}) = 0, \quad X(t=0) = 1 \tag{A.5}$$

$$\hat{D}e\frac{\partial \hat{T}^p_{x'x'}}{\partial t} + \hat{T}^p_{x'x'} = -(2\hat{\beta}X + 2\hat{D}eX\hat{T}^p_{x'x'}) \tag{A.6}$$

$$\hat{D}e\frac{\partial \hat{T}^p_{y'y'}}{\partial t} + \hat{T}^p_{y'y'} = (2\hat{\beta}X + 2\hat{D}eX\hat{T}^p_{y'y'}) \tag{A.7}$$

We numerically solve Eqs. (A.5)–(A.7) with stress initial conditions, as mentioned above, computed from the average simulated stress.

References

[1] A. Luciani, M.F. Champagne, L.A. Utracki, Interfacial tension coefficient from the retraction of ellipsoidal drops, Journal of Polymer Science Part B-Polymer Physics 35 (1997) 1393–1403.
[2] H.Y. Mo, C.X. Zhou, W. Yu, A new method to determine interfacial tension from the retraction of ellipsoidal drops, Journal of Non-Newtonian Fluid Mechanics 91 (2000) 221–232.
[3] Y. Son, J.T. Yoon, Measurement of interfacial tension by a deformed drop retraction method, Polymer 42 (2001) 7209–7213.
[4] S. Guido, M. Villone, Measurement of interfacial tension by drop retraction analysis, Journal of Colloid and Interface Science 209 (1999) 247–250.
[5] G.I. Taylor, The formation of emulsions in definable fields of flow, Proceedings of the Royal Society of London Series A-Mathematical and Physical Sciences 146 (1934) 0501–0523.
[6] G.I. Taylor, The viscosity of a fluid containing small drops of another fluid, Proceedings of the Royal Society of London Series A 138 (1932) 41–48.
[7] J.M. Rallison, The deformation of small viscous drops and bubbles in shear flows, Annual Review of Fluid Mechanics 16 (1984) 45–66.
[8] H.A. Stone, Dynamics of drop deformation and breakup in viscous fluids, Annual Review of Fluid Mechanics 26 (1994) 65–102.
[9] C.E. Chaffey, H. Brenner, A second order theory for shear deformation of drops, Journal of Colloid and Interface Science 24 (1967) 258–269.
[10] B.J. Bentley, L.G. Leal, A computer-controlled 4-Roll Mill for investigations of particle and drop dynamics in two-dimensional linear shear flows, Journal of Fluid Mechanics 167 (1986) 219–240.
[11] B.J. Bentley, L.G. Leal, An experimental investigation of drop deformation and breakup in steady, two-dimensional linear flows, Journal of Fluid Mechanics 167 (1986) 241–283.
[12] A. Acrivos, The breakup of small drops and bubbles in shear flows, Annals of the New York Academy of Sciences 404 (1983) 1–11.
[13] C.L. Tucker, P. Moldenaers, Microstructural evolution in polymer blends, Annual Review of Fluid Mechanics 34 (2002) 177–210.
[14] J.F. Brady, A. Acrivos, The deformation and breakup of a slender drop in an extensional flow—inertial effects, Journal of Fluid Mechanics 115 (1982) 443–451.
[15] K. Sarkar, W.R. Schowalter, Deformation of a two-dimensional drop at non-zero Reynolds number in time-periodic extensional flows: numerical simulation, Journal of Fluid Mechanics 436 (2001) 177–206.
[16] K. Sarkar, W.R. Schowalter, Deformation of a two-dimensional viscous drop in time-periodic extensional flows: analytical treatment, Journal of Fluid Mechanics 436 (2001) 207–230.

[17] X.Y. Li, K. Sarkar, Drop dynamics in an oscillating extensional flow at finite Reynolds numbers, Physics of Fluids 17 (2005) 027103.
[18] X.Y. Li, K. Sarkar, Effects of inertia on the rheology of a dilute emulsion of drops in shear, Journal of Rheology 49 (2005) 1377–1394.
[19] X. Li, K. Sarkar, Negative normal stress elasticity of emulsion of viscous drops at finite inertia, Physical Review Letters 95 (2005) 256001.
[20] X.Y. Li, K. Sarkar, Drop deformation and breakup in a vortex at finite inertia, Journal of Fluid Mechanics 564 (2006) 1–23.
[21] D.R. Mikulencak, J.F. Morris, Stationary shear flow around fixed and free bodies at finite Reynolds number, Journal of Fluid Mechanics 520 (2004) 215–242.
[22] G. Subramanian, D.L. Koch, Inertial effects on the orientation of nearly spherical particles in simple shear flow, Journal of Fluid Mechanics 557 (2006) 257–296.
[23] E.M. Toose, B.J. Geurts, J.G.M. Kuerten, A boundary integral method for 2-dimensional (non)-Newtonian drops in slow viscous-flow, Journal of Non-Newtonian Fluid Mechanics 60 (1995) 129–154.
[24] K. Sarkar, W.R. Schowalter, Deformation of a two-dimensional viscoelastic drop at non-zero Reynolds number in time-periodic extensional flows, Journal of Non-Newtonian Fluid Mechanics 95 (2000) 315–342.
[25] D.C. Tretheway, L.G. Leal, Deformation and relaxation of Newtonian drops in planar extensional flows of a Boger fluid, Journal of Non-Newtonian Fluid Mechanics 99 (2001) 81–108.
[26] S. Ramaswamy, L.G. Leal, The deformation of a viscoelastic drop subjected to steady uniaxial extensional flow of a Newtonian fluid, Journal of Non-Newtonian Fluid Mechanics 85 (1999) 127–163.
[27] D. Khismatullin, Y. Renardy, M. Renardy, Development and implementation of VOF-PROST for 3D viscoelastic liquid–liquid simulations, Journal of Non-Newtonian Fluid Mechanics 140 (2006) 120–131.
[28] V. Sibillo, M. Simeone, S. Guido, Break-up of a Newtonian drop in a viscoelastic matrix under simple shear flow, Rheologica Acta 43 (2004) 449–456.
[29] K. Verhulst, R. Cardinaels, P. Moldenaers, Y. Renardy, S. Afkhami, Influence of viscoelasticity on drop deformation and orientation in shear flow. Part 1. Stationary states, Journal of Non-Newtonian Fluid Mechanics 156 (2009) 29–43.
[30] P.T. Yue, J.J. Feng, C. Liu, J. Shen, Viscoelastic effects on drop deformation in steady shear, Journal of Fluid Mechanics 540 (2005) 427–437.
[31] R.W. Hooper, V.F. de Almeida, C.W. Macosko, J.J. Derby, Transient polymeric drop extension and retraction in uniaxial extensional flows, Journal of Non-Newtonian Fluid Mechanics 98 (2001) 141–168.
[32] W. Yu, M. Bousmina, C.X. Zhou, C.L. Tucker, Theory for drop deformation in viscoelastic systems, Journal of Rheology 48 (2004) 417–438.
[33] S.B. Pilapakkam, P. Singh, A level-set method for computing solutions to viscoelastic two-phase flow, Journal of Computational Physics 174 (2004) 552–578.
[34] R.W. Flumerfelt, Drop breakup in simple shear fields of viscoelastic fluids, Industrial & Engineering Chemistry Fundamentals 11 (1972) 312–318.
[35] J.J. Elmendorp, R.J. Maalcke, A study on polymer blending microrheology. 1, Polymer Engineering and Science 25 (1985) 1041–1047.
[36] F. Mighri, A. Ajji, P.J. Carreau, Influence of elastic properties on drop deformation in elongational flow, Journal of Rheology 41 (1997) 1183–1201.
[37] F. Mighri, P.J. Carreau, A. Ajji, Influence of elastic properties on drop deformation and breakup in shear flow, Journal of Rheology 42 (1998) 1477–1490.
[38] S. Guido, M. Simeone, F. Greco, Effects of matrix viscoelasticity on drop deformation in dilute polymer blends under slow shear flow, Polymer 44 (2003) 467–471.
[39] P.L. Maffettone, F. Greco, Ellipsoidal drop model for single drop dynamics with non-Newtonian fluids, Journal of Rheology 48 (2004) 83–100.
[40] N. Aggarwal, K. Sarkar, Effects of matrix viscoelasticity on viscous and viscoelastic drop deformation in a shear flow, Journal of Fluid Mechanics 601 (2008) 63–84.
[41] N. Aggarwal, K. Sarkar, Deformation and breakup of a viscoelastic drop in a Newtonian matrix under steady shear, Journal of Fluid Mechanics 584 (2007) 1–21.
[42] N. Aggarwal, K. Sarkar, Rheology of an emulsion of viscoelastic drops in steady shear, Journal of Non-Newtonian Fluid Mechanics 150 (2008) 19–31.
[43] S. Mukherjee, K. Sarkar, Effects of viscosity ratio on deformation of a viscoelastic drop in a Newtonian matrix under steady shear, Journal of Non-Newtonian Fluid Mechanics 160 (2009) 104–112.
[44] V. Sibillo, M. Simeone, S. Guido, F. Greco, P.L. Maffettone, Start-up and retraction dynamics of a Newtonian drop in a viscoelastic matrix under simple shear flow, Journal of Non-Newtonian Fluid Mechanics 134 (2006) 27–32.
[45] P.T. Yue, J.J. Feng, C. Liu, J. Shen, Diffuse-interface simulations of drop coalescence and retraction in viscoelastic fluids, Journal of Non-Newtonian Fluid Mechanics 129 (2005) 163–176.
[46] K. Verhulst, R. Cardinaels, P. Moldenaers, S. Afkhami, Y. Renardy, Influence of viscoelasticity on drop deformation and orientation in shear flow. Part 2. Dynamics, Journal of Non-Newtonian Fluid Mechanics 156 (2009) 44–57.
[47] H.A. Stone, L.G. Leal, The influence of initial deformation on drop breakup in subcritical time-dependent flows at low Reynolds-numbers, Journal of Fluid Mechanics 206 (1989) 223–263.